The Inhomogeneous Chemical Evolution of the Carina Dwarf Galaxy

Venn, K.; Lemasle, B.; Shetrone, M.; Hill, V.; Tolstoy, E.; Irwin, M.

The Inhomogeneous Chemical Evolution of the Carina Dwarf Galaxy

Kim Venn,[1] Bertrand Lemasle,[2] Matthew Shetrone,[3] Vanessa Hill,[4] Eline Tolstoy,[2] Mike Irwin [5]

[1]*University of Victoria, Dept. of Physics & Astronomy, Elliott Building, 3800 Finnery Road, Victoria, BC, V8P 5C2, CANADA*

[2] *Kapteyn Astronomical Institute, University of Groningen, PO Box 800, 9700AV Groningen, The Netherlands*

[3] *McDonald Observatory, University of Texas at Austin, HC75 Box 1337-MCD, Fort Davis, TX, 79734*

[4] *Université de Nice Sophia-Antipolis, CNRS, Observatoire de la Côte d'Azur, Laboratoire Cassiopée, 06304, Nice Cedex 4, France*

[5] *Institute of Astronomy, University of Cambridge, Madingley Road, Cambridge CB3 0HA, UK*

1. Introduction

The Carina dSph galaxy has long been known to have an unusual and episodic star formation history, with distinct main sequence turnoffs clearly seen in its deep colour magnitude diagram (first shown by Smecker-Hane et al. 1996). Its star formation history is best described by an old population (10-12 Gyr), a dominant intermediate-aged population ($\sim$ 75% with ages 5-7 Gyr), and a trace young population (1-2 Gyr), separated by long quiescent periods (e.g., Bono et al. 2010, Lanfranchi et al. 2006, Monelli et al. 2003, Dolphin 2002). In spite of this punctuated star formation history, the Carina dSph has a very narrow red giant branch, most likely due to a fortuitous alignment in the age-metallicity degeneracy, but also partially due to the fact that the majority of stars are from the intermediate-aged population which may have a very small metallicity spread (Bono et al. 2010).

VLT FLAMES multi-fiber spectroscopy has been carried out for red giant branch stars in the inner region of the Carina dwarf galaxy. High resolution (R~45,000) UVES spectroscopy over a 2000 Å range has been obtained for 17 stars (Venn et al. 2012, Koch et al. 2008, Shetrone et al. 2003), while GIRAFFE (R~20,000) spectroscopy has been examined for an additional 35 stars over three shorter wavelength intervals (totalling ~700Å; Lemasle et al. 2012). In addition to this, we have obtained high resolution (R~30,000) spectroscopy with the MIKE spectrograph at the Magellan telescope for three stars in the outer fields of Carina. The Magellan spectra also have the advantage of extending to very blue wavelengths (~3800 Å) where spectral lines of additional elements are located.

2. Metallicities

The metallicities of all of the stars observed spectroscopically are shown in Fig. 1. This includes over 400 RGB stars with metallicities determined from the Ca II triplet (Koch et al. 2006, Starkenburg et al. 2010), and 20 RGB stars with high resolution spectroscopic analyses by Venn et al. (2012), Lemasle et al. (2012), Koch et al. (2008), and Shetrone et al. (2003). The mean metallicity of the stars with high resolution spectroscopic analyses is higher than mean metallicity of the full distribution function; however this is most likely an observational bias. The only target selection criteria used in these projects were that the stars needed to be bright, red giants, and members of the Carina dSph. The slightly higher V magnitude associated with higher metallicities at the RGB tip may have contributed to the specific selections, but cannot have had a major effect since maximizing fiber placement was also a concern. Furthermore, while the three Magellan targets are located in the outer fields of Carina, they were purposely selected for their low metallicities, and therefore cannot be used (on their own) to suggest whether there is a population gradient between the inner and outer fields in Carina. Koch et al. (2006) found no significant difference in the mean metallicity of stars located in the inner versus outer fields of Carina. That the median metallicity ($\pm\sigma$) of the high resolution sample is the same as the mean metallicity predicted by Bono et al. (2010) for the intermediate aged population is interesting but not scientifically significant given our small sample.
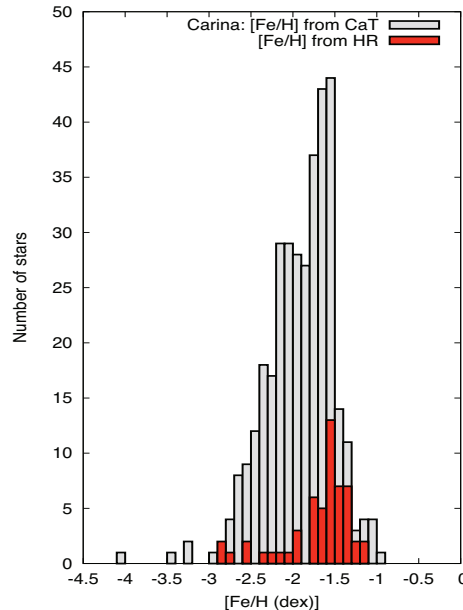

Figure 1.   The [Fe/H] distribution of RGB stars in the Carina dSph. Metallicities for > 400 stars based on the CaT are shown in grey (Koch et al. 2006, Starkenburg et al. 2010), and those with high resolution spectroscopic metallicities are shown in red (Venn et al. 2012, Lemasle et al. 2012, Koch et al. 2008, and Shetrone et al. 2003).

3. Abundance Ratios

The abundances of up to 23 elements in 20 RGB stars are now available in the Carina dSph from high resolution, large wavelength coverage, spectroscopic analyses. A representative sample of elements are shown in Fig. 2 (the full sample is presented in Venn et al. 2012). In Fig. 2, the abundance ratios for these stars are separated into two age groups (old = red, young = blue). Ages are determined from isochrone fitting by Lemasle et al. (2012), accounting for the [Fe/H] and [α/Fe] determinations per star. The overlap in the [Mg/Fe] ratios at intermediate metallicities was interpreted by Lemasle et al. (2012) as evidence for infall of α-enriched metal-poor gas to trigger the second epoch of star formation in the Carina dSph.

The dispersion in the [Mg/Fe] ratios is larger than has been found in any other dSph galaxy, in particular stars in the Carina dSph show the lowest values of [Mg/Fe] yet found for their metallicities. In Car-5070 and other metal poor stars with [Fe/H]< −2, the low [Na/Fe] and [Mn/Fe] (also some neutron capture elements) suggest that these stars have *not* been enhanced by SNe Ia (Cescutti et al. 2008, Kobayashi & Nomoto 2009), nor by AGB stars (Herwig et al. 2004, Karakas 2010). This is important since a decrease in [α/Fe] with increasing [Fe/H] is usually interpreted as evidence for contributions from SNe Ia. In fact, the *knee* in this ratio is interpreted as the metallicity when SNe Ia begin to contribute to the chemical evolution of a galaxy (Tolstoy et al. 2009), however this only applies to simple homogeneous closed/leaky box models, which does not appear to be the case for Carina. The dispersion in [Mg/Fe] and other higher order abundance ratios, particularly in the old population, is more consistent with inhomogeneous mixing of the interstellar gas and stochastic statistical sampling of the SNe II yields during the formation of individual stars (e.g., Revaz & Jablonka 2011).

In addition, low [Mn/Fe] ratios and the low [Zn/Fe] limit for Car-5070 suggest that the metal poor stars may have formed from gas that is lacking contributions from hypernovae (Kobayashi & Nomoto 2009, Heger & Woosley 2010). This is further supported by the neutron capture ratios (see Venn et al. 2012) and suggests that the most massive SNe II progenitors did not form or that their gas was driven out in the SN II explosion. We also note that the chemistry of one star, Car-612 (labelled in Fig. 2) is very unusual, e.g., showing underabundances of nearly all ratios relative to iron, [X/Fe] (including Ni, but not Mn). We propose that this star has an overabundance of SN Ia/SN II contributions by a factor ~5. Peculiar chemical abundances can affect the ages from isochrone fitting (Dotter et al. 2007), and so Car-612's age should be considered highly uncertain. If this star is younger than 10 Gyr, then this would significantly reduce the overlap in metallicity between the *old* and *intermediate aged* populations found by Lemasle et al. (2012). It may even suggest that the second epoch of star formation did arise from the existing chemically enriched gas, most likely an α-rich pocket, e.g., in the central region.

References

Bono, G., et al. 2010, PASP, 122, 651
Cescutti, G., Matteucci, F., Lanfranchi, G. A., & McWilliam, A. 2008, A&A, 491, 401
Dolphin A.E., 2002, MNRAS, 332, 91
Dotter A., et al. 2007, ApJ, 666, 403
Frebel A., 2010, Astronomische Nachrichten, 331, 474
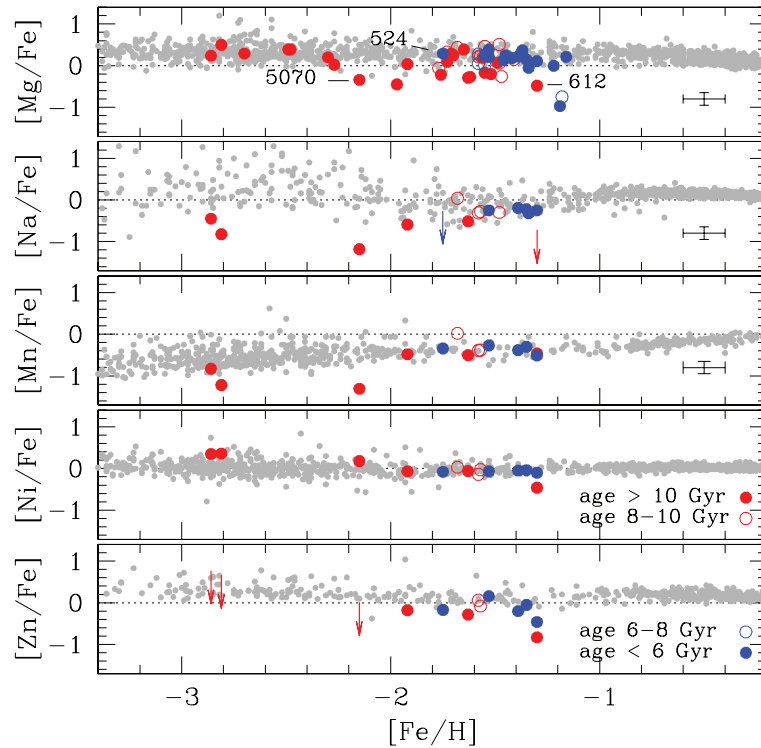Herwig F., 2004, ApJS, 155, 651

Figure 2.   (color online) Abundance ratios for stars in the Carina dSph separated into two age groups: stars >10 Gyr old are represented by red filled circles, stars <6 Gyr are respresented by blue filled circles. Stars at intermediate age ranges are represented by open circles (6−8 Gyr are blue, 8−10 Gyr are red). Carina abundance data is from Venn et al. (2012), Lemasle et al. (2012), Koch et al. (2008), and Shetrone et al. (2003); ages are from Lemasle et al. (2012). Galactic comparison stars are shown as small grey dots (including data from Venn et al. 2004, Frebel et al. 2010, Reddy et al. 2003, 2006).

Karakas A., 2010, MNRAS, 403, 1413

Karakas A., Lee H.Y., Lugaro M., Görres J., & Wiescher M., 2008, ApJ, 676, 1254

Kobayashi, C., & Nomoto, K. 2009, ApJ, 707, 1466

Koch A., Grebel E.K., Wyse R.F.G., Kleyna J.T., Wilkinson, M.I., Harbeck D.R., Gilmore G.F., & Evans N.W., 2006, AJ, 131, 895

Koch A., Grebel E.K., Gilmore G.F., Wyse R.F.G., Kleyna J.T., Harbeck D.R., Wilkinson M.I., Wyn & Evans, N., 2008, AJ, 135, 1580

Lanfranchi, G. A., Matteucci, F., & Cescutti, G. 2006, A&A, 453, 67

Lemasle B., et al. 2012, A&A, in press

Monelli M., Pulone L., Corsi C.E., Castellani M., et al. 2003 AJ, 126, 218

Reddy, B. E., Lambert, D. L., & Allende Prieto, C. 2006, MNRAS, 367, 1329

Reddy, B. E., Tomkin J., Lambert, D. L., & Allende Prieto, C. 2003, MNRAS, 340, 304

Revaz Y., & Jablonka P., 2011, A&A, in press

Shetrone M.D., Venn K.A., Tolstoy E., Primas F., Hill V., & Kaufer A., 2003, AJ, 125, 684

Smecker-Hane T.A., Stetson P.B., Hesser J.E., & Lehnert M.D., 1994, AJ, 108, 507

Starkenburg E., et al., 2010 A&A, 513, 34

Venn K.A., et al. 2012, ApJ, submitted

Venn K.A., Irwin M.J., Shetrone M.D., Tout C.A., Hill V., Tolstoy E., 2004 AJ, 128, 1177